Short Communication

Electrocatalytic Oxidation of Formic Acid at Manganese Oxide Nanorods Modified Electrodes: Effect of Substrate

Mohamed S. El-Deab[1,2,], Takeo Ohsaka[1,*]*

[1] Department of Electronic Chemistry, Interdisciplinary Graduate School of Science and Engineering, Tokyo Institute of Technology, 4259 Nagatsuta, Midori-ku, Yokohama 226-8502, Japan
[2] Department of Chemistry, Faculty of Science, Cairo University, Cairo, Egypt
*E-mail: msaada68@yahoo.com; ohsaka@echem.titech.ac.jp

Electrochemical oxidation of formic acid (FA) has been investigated at manganese oxide nanorods (nano-MnOx) modified electrodes (i.e., Au, Pt, GC and Pd). The electrocatalytic activity of the aforementioned anodes depends markedly on the nature of the underlying substrate. That is, the nano-MnOx at Pt electrode enhances the direct oxidation of FA. However, it does not show any significant enhancing effect on the poor catalytic activity of Au and GC electrodes. The catalytic role of nano-MnOx is inherently connected with a substrate suitable for FA adsorption (case of Pt, but not Au or GC) and/or the generation of a poisoning CO intermediate (case of Pt but not Pd, Au or GC). At Pt electrode, nano-MnOx facilitates the electrooxidation of the generated poisoning CO intermediate at a reasonably low anodic potential, while it does not affect the catalytic activity of Pd electrode towards the direct oxidation of FA to CO_2 (which occurs with no CO formation).

1. INTRODUCTION

Formic acid (FA) is one of the promising fuels in polymer electrolyte membrane fuel cells (PEMFCs). It is a cheap material which has a high energy density [1-3], in addition to its low affinity to crossover compared to methanol fuel cell [4,5]. The oxidation of FA is shown to proceed via various pathways [6-9] including (i) dehydrogenation (direct) pathway producing CO_2 and (ii) dehydration (indirect) pathway producing the poisoning CO intermediate. Several strategies have been suggested to promote the direct oxidation pathway at the expense of the CO formation. This includes the use of

anodes fabricated from various metallic (mostly Pt-based alloys) and/or metal oxide nanostructures with a high ability to oxidize FA to CO_2 [1,10-12].

In this context, materials in a highly dispersed form have found numerous applications in the areas of catalysis and electrocatalysis where advantage is taken of their high surface to volume ratio to increase overall performance, while minimizing costs of often expensive metal and alloy constituents [13]. For instance, electrodes modified with metal oxide (e.g., MnOx, Fe_3O_4, Co_3O_4, or NiOx) nanostructures with various morphologies (e.g., nanotubes, nanorods and nanoparticles [11-12]) have revealed superior electrocatalytic activity towards the oxygen reduction reaction (ORR), water electrolysis, catalytic hydrogenation of unsaturated alcohols and aldehydes as well as the electro-oxidation of methanol and formic acid [14-18].

In the present study, we investigate the effect of the nature of the underlying substrate on the electrocatalytic activity of manganese oxide nanorods (nano-MnOx) towards FA oxidation. Nano-MnOx has been electrodeposited onto various substrates, typically Au, GC, Pt and Pd electrodes and their electrocatalytic activity towards FA oxidation has been examined.

2. EXPERIMENTAL

Polycrystalline Pt, Pd and Au electrodes (d = 1.6 mm) and GC (d = 3.0 mm) were used as the working electrodes. Spiral Pt wire and a SCE were used as the counter and the reference electrodes, respectively. The working (Pt, Pd, Au and GC) electrodes were mechanically polished with aqueous slurries of successively finer alumina powder (particle size down to 0.06 μm) with the help of a polishing microcloth and sonicated for 10 min in Milli-Q water. Moreover, Pt, Au and Pd electrodes were further electrochemically pretreated in N_2-saturated 0.1 M H_2SO_4 solution by cycling the potential between the onset of the hydrogen evolution and oxygen evolution reaction i.e., –0.25 and 1.25 V for Pt and –0.25 and 1.45 V for Au, at 100 mV s^{-1} for 10 min or until a reproducible cyclic voltammograms (CVs) characteristic of clean Pt, Au and Pd electrodes were obtained (cf., Fig. 1B, curve *a* for a clean Pt electrode).
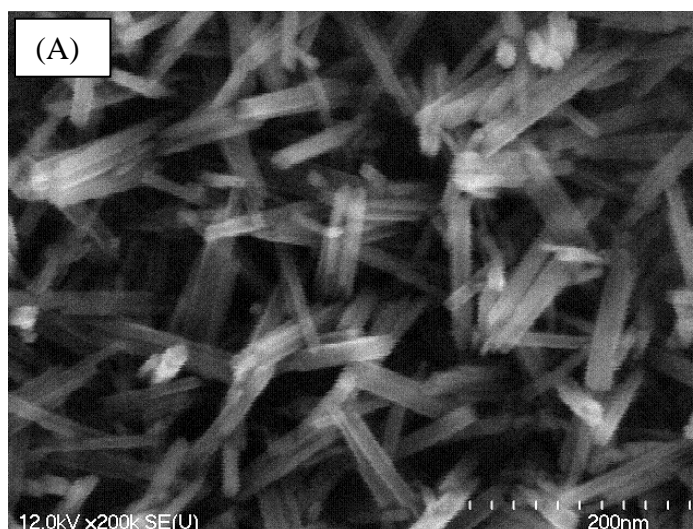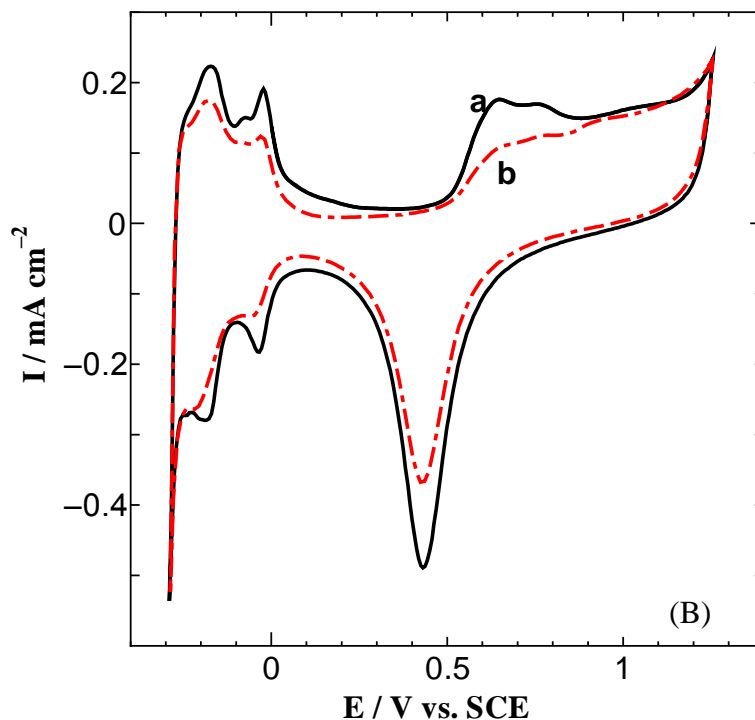
Figure 1. (A) SEM micrograph of nano-MnOx modified Pt electrode. (B) CVs for (a) unmodified and (b) nano-MnOx modified ($\theta = 0.3$) Pt electrodes measured in N_2-saturated 0.1 M H_2SO_4 at 50 mV s^{-1}. The nano-MnOx was electrodeposited as described in the experimental section employing 25 potential cycles between −50 and 350 mV vs. SCE at 20 mV s^{-1}.

Nano-MnOx was electrodeposited on the surface of the thus-pretreated Pt, Au, Pd and GC electrodes from an aqueous solution of 0.1 M Na_2SO_4 containing 0.1 M $Mn(CH_3COO)_2$ by cycling the potential between −50 mV and 350 mV vs. SCE at 20 mV s^{-1} several times [19]. The surface coverage (θ) [20] of the nano-MnOx was controlled by the number of potential cycles employed during the electrodeposition.

The thus-prepared nano-MnOx modified electrodes were electrochemically characterized by measuring the characteristic CVs in N_2-saturated 0.1 M H_2SO_4 from which the real surface areas of the unmodified and nano-MnOx modified Pt electrodes were estimated [20,21]. Whereas, the morphological characterization of the prepared catalysts was carried out by scanning electron microscopy (SEM) using a JSM-T220 (JEOL, Optical Laboratory, Japan) at an acceleration voltage of 12 kV and a working distance of 4-5 mm.

3. RESULTS AND DISCUSSION

3.1. Characterization of nano-MnOx modified electrodes

Fig. 1(A) shows a typical example of SEM images of nano-MnOx modified surfaces. It shows that intersected MnOx nanorods are electrodeposited onto Pt electrode in a porous texture leaving a fraction of its surface uncovered. Similar geometries were also observed for nano-MnOx
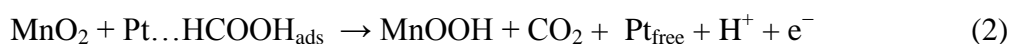
electrodeposited onto Au, GC and Pd electrodes. Fig. 1(B) shows a typical characteristic cyclic voltammetric (CV) response of (a) unmodified and (b) nano-MnOx modified Pt electrodes measured in 0.1 M H_2SO_4. This figure shows that the Pt oxide reduction peak (at ca. 0.4 V) is observed with lower current, upon the modification of Pt with nano-MnOx (curve b). This indicates the partial coverage of Pt with nano-MnOx with a surface coverage (θ) of 0.3. Furthermore, phase characterization of the electrodeposited nano-MnOx has been performed employing high resolution TEM and XRD techniques (data are shown elsewhere [16,22]). Both techniques revealed the electrodeposition of MnOx nanorods in a manganite phase (γ-MnOOH). Furthermore, XPS data have been collected (data shown elsewhere [16,23,24]) and indicated the absence of any electronic interaction between nano-MnOx and the underlying substrate.

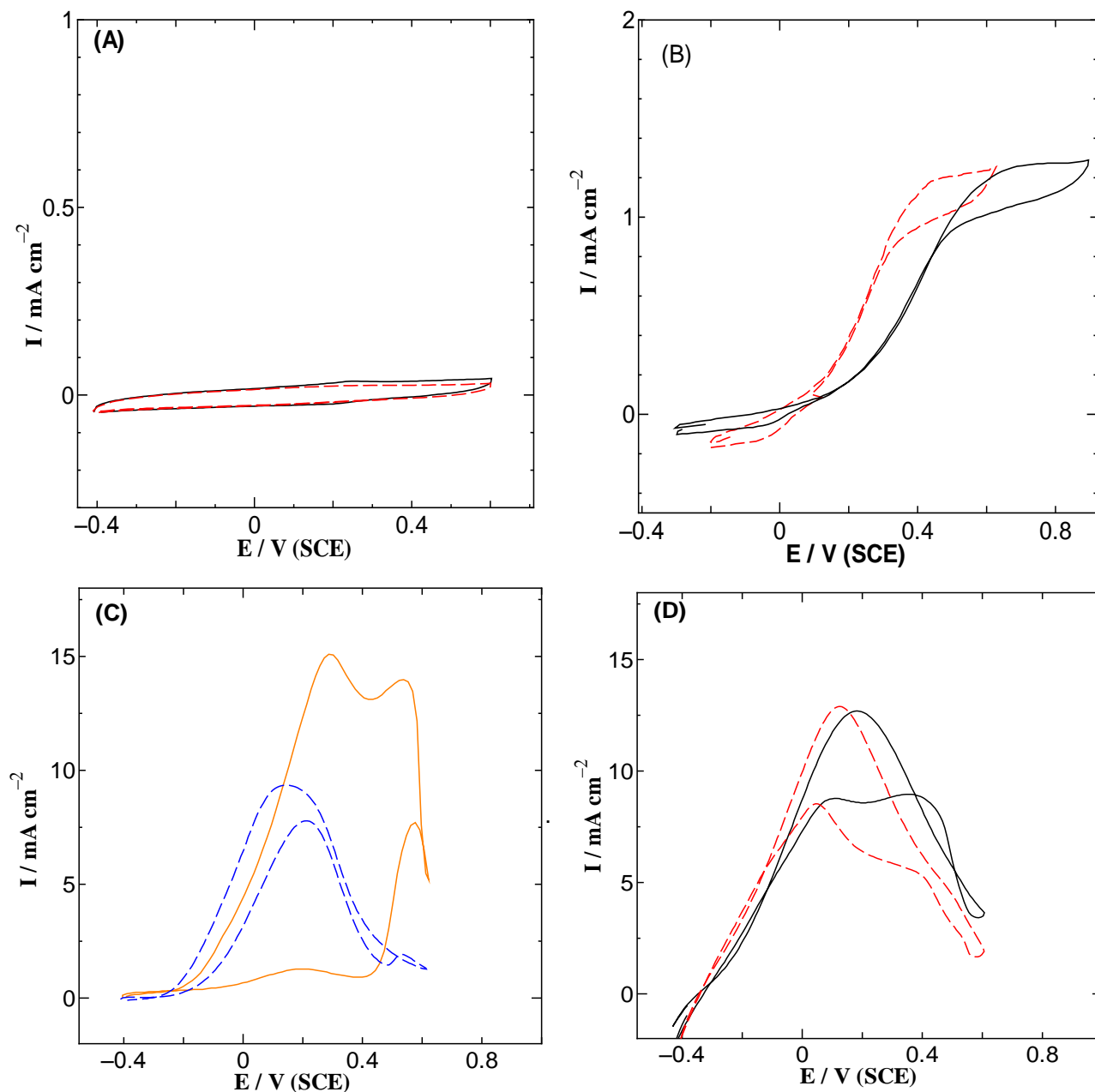### 3.2. Formic acid oxidation

Fig. 2 shows CVs measured at unmodified (solid lines) and nano-MnOx modified (dashed lines) (A) GC, (B) Au, (C) Pt and (D) Pd electrodes in an aqueous solution of 0.3 M FA (pH 3.5) at a potential scan rate of 50 mV s^{-1}. Inspection of this figure reveals that neither unmodified nor nano-MnOx modified GC electrodes show any significant catalytic activity towards FA oxidation (panel A). A similar behavior is observed at Au electrodes with/without nano-MnOx modification (shown in panel B) where an oxidation wave is observed – albeit with a negligible peak current as small as 1 mA cm^{-2} – at unmodified Au (solid curve, panel B). Upon the modification with nano-MnOx (dashed curve, panel B), the peak potential shifts only slightly towards less anodic values without any noticeable increase of the peak current which is still far smaller than that observed at catalytic surfaces (cf. panel C). On the contrary, unmodified Pt electrode showed two oxidation peaks of FA at ca. 0.2 and 0.6 V vs. SCE (albeit with unequal peak current intensities, solid curve in panel C) which are frequently attributed to the direct oxidation of FA to CO_2 and the oxidation of the poisoning intermediate CO (produced at the Pt surface as a result of the "*non-faradaic*" dissociation of FA) to CO_2, respectively [21,25]. The modification of Pt with nano-MnOx resulted in a significant enhancement of the direct oxidation at the expense of the indirect one, as can be evident by comparing the current intensities of the two oxidation peaks shown in the dashed curve of panel C. This observation has been accounted for by the catalytic mediation of FA oxidation by nano-MnOx via a reversible redox reaction of the $MnOOH/MnO_2$ couple [17,21,26] as:

$$MnOOH = MnO_2 + H^+ + e^- \tag{1}$$

Hence, the strongly oxidizing MnO_2 facilitates the oxidation of the adsorbed formic acid and/or CO to CO_2 as:

$$MnO_2 + Pt\ldots HCOOH_{ads} \rightarrow MnOOH + CO_2 + Pt_{free} + H^+ + e^- \tag{2}$$

$$MnO_2 + Pt\ldots CO_{ads} + H_2O \rightarrow MnOOH + CO_2 + Pt_{free} + H^+ + e^- \tag{3}$$
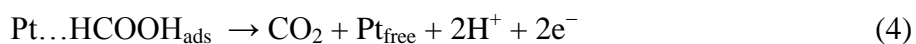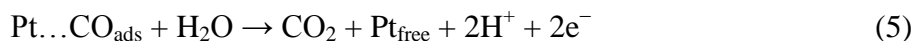
where the terms "Pt…HCOOH$_{ads}$" and "Pt…CO$_{ads}$" refer to FA and CO molecules adsorbed at Pt active surface sites, respectively. It is worthy mentioning here that CO is produced at Pt surface via a *"non-faradaic"* dissociation (HCOOH = H$_2$O + CO$_{ads}$).

Figure 2. CVs for FA oxidation at unmodified (solid lines) and nano-MnOx modified (dashed lines) (A) GC, (B) Au, (C) Pt and (D) Pd electrodes measured in 0.3 M FA (pH 3.5) at 50 mV s^{-1}.

The sequential coupling of Reactions (1) and (2) or (3) results in the formation of CO$_2$ and the retrieval of free Pt active surface sites:

$$\text{Pt…HCOOH}_{ads} \rightarrow CO_2 + \text{Pt}_{free} + 2H^+ + 2e^- \qquad\qquad (4)$$

$$Pt \ldots CO_{ads} + H_2O \rightarrow CO_2 + Pt_{free} + 2H^+ + 2e^- \qquad (5)$$

On the other hand, FA oxidation to CO_2 proceeds with no CO formation at unmodified Pd electrode via a single oxidation peak observed at ca. 0.1 V vs. SCE (solid curve, panel D), similar to previous reports [27]. Surprisingly, the modification of Pd electrode with nano-MnOx does not enhance the peak current but a slight negative shift of the peak potential is observed (dashed curve, panel D). This observation indicates that the rate of the direct FA oxidation at Pd electrode is not significantly accelerated with nano-MnOx. Thus, one can safely argue that the major catalytic role of nano-MnOx (in case of modified Pt) might be attributed to the oxidative removal of the adsorbed poisoning CO intermediate leading to the retrieval of active Pt sites (see Reaction 3 above), rather than enhancing the direct FA oxidation (Reaction 2).

It is generally accepted that the adsorption of FA on the electrode surface is the first step in its electro-oxidation. FA is a weak electrolyte which is not capable of getting adsorbed on Au surface. For instance, it is a weak ligand which can hardly replace the citric/citrate sheath covering the citrate-stabilized Au nanoparticles [28]. It is worthy mentioning here that the dehydration of FA to CO_{ads} necessitates at least three adjacent Pt atoms, whereas the dehydrogenation path requires at most two Pt atoms [29]. On the other hand, the favorable adsorption geometry of the surface atoms is missing in the case of Au and GC surfaces possibly due to the higher electronegativity of Au than Pt along with the larger lattice constant of Au than that of Pt, although these both parameters lead to the stronger adsorption of FA (and/or CO) on Pt [29-33]. The weak adsorption of FA at Au is thought as the main reason for the absence of any catalytic role of nano-MnOx at Au electrode. Thus, the nature of the underlying substrate and its affinity to FA adsorption determine to a large extent its oxidation pathway, i.e., either via a direct oxidation to CO_2 or via the formation of a poisoning CO intermediate and subsequently the role of nano-MnOx comes next. In other words, the superior enhancement of nano-MnOx is inherently connected with the nature of the substrate not only with a high affinity towards FA adsorption (like Pt and Pd) but also with a high capability to produce the *"non-faradaic"* poisoning intermediate (i.e., CO) which is the case of Pt.

4. CONCLUSION

The enhancement of the electrocatalytic activity of nano-MnOx towards FA oxidation at various substrates is investigated. Nano-MnOx exerts its catalytic enhancing role via facilitating the oxidation of the adsorbed poisoning intermediate of CO to CO_2, thus generating free active Pt sites suitable for FA adsorption (which is an essential step in its oxidation process). The absence of any catalytic role of nano-MnOx at Pd electrode is attributed to the direct oxidation of formic acid to CO_2 at both unmodified and nano-MnOx-modified Pd electrodes (which occurs with no CO formation). On the other hand, the modified Au and GC electrodes did not show any significant catalytic enhancement towards FA oxidation possibly due to the lack of suitable adsorption sites for FA at both electrode surfaces.

References

1. N. Kristian, Y. Yan, X. Wang, *Chem. Commun*. (2008) 353.
2. S. Chen, D. Lee, M. Schell, *Electrochim. Acta* 46 (2001) 48.
3. Z. Zhang, Y. Huang, J. Ge, C. Liu, T. Lu, W. Xing, *Electrochem. Commun*. 10 (2008) 1113.
4. U. B. Demirci, *J. Power Sources*, 169 (2007) 239.
5. X. Wang, J. M. Hu, I. M. Hsing, *J. Electroanal. Chem*., 562 (2004) 73.
6. J.D. Lovic, A.V. Tripkovic, S. Lj, K.Dj. Gijkovic, D.V. Popovic, P. Tripkovic, A. Kowal, *J. Electroanal. Chem*. 581 (2005) 294.
7. J.M. Feliu, E. Herrero, in: W. Vielstich, H.A. Gasteiger, A. Lamm (Eds.), Handbook of Fuel Cells, vol. 2, Wiley, New York, 2003, p. 625.
8. A.Capon, R. Parson, *J. Electroanal. Chem*. 44 (1973) 239.
9. N.M. Markovic, P. Ross, *Surf. Sci. Rep*. 45 (2002) 117.
10. W. Chen, J. Kim, S. Sun, S. Chen, *Langmuir*, 23 (2007) 11303.
11. F. Kim, J. H. Song, P. Yang, *J. Am. Chem. Soc.,* 124 (2002) 14316.
12. N. Malikova, I. P. Santos, M. Schierhorn, N. A. Kotov, L. M. L. Marzan, *Langmuir*, 18 (2002) 3694.
13. "Catalysis and Electrocatalysis at Nanoparticle Surfaces" A. Wieckowski, E. R. Savinova and C. G. Vayenas (Eds.), Marcel Dekker, Inc., New York (2003).
14. M.-W. Xu, G.-Y. Gao, W.-Y. Zhou, K.-F. Zhang, H.-L. Li, *J. Power Sources* 175 (2008) 217.
15. M. S. El-Deab, T. Ohsaka, *J. Electrochem. Soc*., 153 (2006) A1365.
16. M. S. El-Deab, T. Ohsaka, *Angew. Chem. Int. Ed*., 45 (2006) 5963.
17. M. S. El-Deab, *Int. J. Electrochem. Sci*., 4 (2009) 1329.
18. I.M. Sadiek, A. M. Mohammad, M. E. El-Shakre, M. S. El-Deab, *Int. J. Hydrogen Energy*, 37 (2012) 68.
19. M.-S. Wu, P.-C.J. Chiang, Electrochem. *Solid-State Lett*., 7 (2004) A123.
20. S. Trasatti, O.A. Petrii, *Pure Appl. Chem*., 63 (1991) 711.
21. M. S. El-Deab, L. A. Kibler, D. M. Kolb, *Electrochem. Commun*., 11 (2009) 776.
22. M. S. El-Deab, T. Ohsaka, *J. Electrochem. Soc*. 155 (2008) D14.
23. A.M. Mohammad, M. I. Awad, M. S. El-Deab, T. Okajima, T. Ohsaka, *Electrochim. Acta*, 53 (2008) 4351.
24. M. S. El-Deab, S. H. Othman, T. Okajima, T. Ohsaka, *J. Appl. Electrochem*., 38 (2008) 1445.
25. J. Masud, M. T. Alam, M. R. Miah, T. Okajima, T. Ohsaka, *Electrochem. Commun*., 13 (2011) 86.
26. M. S. El-Deab, L. A. Kibler, D. M. Kolb, *Electrocatal*., 2 (2011) 220.
27. L.A. Kibler, A.M. El-Aziz, D.M. Kolb, *J. Mol. Catal. A: Chem*. 199 (2003) 57.
28. Y.-R. Zhang, Y.-Z. Xu, Y. Xia, W. Huang, F.-A. Liu, Y.-C. Yang, Z.-L. Li, *J. Colloid Interface* Sci., 359 (2011) 536.
29. A.Cuesta, M. Escudero, B. Lanova, H. Baltruschat, *Langmuir* 25 (2009) 6500.
30. G. Chen, Y. Li, D. Wang, L. Zheng, G. You, C.-J. Zhong, L. Yang, F. Cai, J. Cai, B. H. Chen, *J. Power Sources*, 196 (2011) 8323.
31. J. Greeley, J. K. Norskov, M. Mavrikakis, *Annu. Rev. Phys. Chem*., 53 (2002) 319.
32. B. Hammer, J. K. Norskov, *Adv. Catal*., 45 (2000) 71.
33. C. Berg, H. J. Venvik, F. Strisland, A. Ramstad, A. Borg, *Surf. Sci*., 409 (1998) 1.